

1 Recognizing microplastic deposits on sandy beaches by altimetric positioning, μ -Raman 2 spectroscopy, and multivariate statistical models

3
4 **Abstract:** This study investigates microplastic (MP) pollution along the coast of São Paulo State,
5 southeastern Brazil. We utilized a five-step methodology: geodetic survey, analysis of beach
6 morphometric parameters, beach sediment collection, μ -RAMAN spectrometry for polymer
7 identification, and multivariate statistical models. The coastline was divided into six compartments
8 (C1 to C6) for MP sample collection. Higher MP concentrations were found in C3 and C2, likely
9 influenced by industrial and port activities. Various types of MP, such as pellets, fragments, and
10 fibers, showed distinct distribution patterns due to their sources, intrinsic properties like shape and
11 density, and emission and deposition processes. Fragments and foams were the most common,
12 representing 42% and 35% of the 1,026 MP items found. Statistical tests revealed significant
13 associations between MP types and beach morphometric characteristics, with higher elevations
14 correlating with higher MP concentrations, particularly for pellets and foams. Beaches with
15 intermediate profiles and those facing the southern quadrant tended to accumulate more MPs. The
16 study highlights the complexity of MP dynamics in coastal environments, emphasizing the
17 importance of considering beach physical characteristics, MP type diversity, and local human
18 activities. Identifying areas prone to MP accumulation is crucial for developing specific
19 monitoring and environmental remediation strategies. These strategies align with the peculiarities
20 of each coastal region and contribute to Sustainable Development Goal 14 (Life Below Water)
21 related to ocean health. The practical applications of this research contribute to the development
22 of more effective plastic waste management and containment systems, and the design of specific
23 monitoring and environmental remediation strategies that consider the unique characteristics of
24 each coastal region.

25 26 1. Introduction

27 According to GESAMP (2019), microplastics (MP) are defined as plastic particles less than
28 5 mm in diameter. This definition aims to harmonize monitoring methods and reduce ambiguities,
29 as it is widely used in national and regional programs. As emerging pollutants on sandy beaches,
30 MPs reduce their aesthetic value, affecting their visual appeal and the recreational quality of these
31 environments (Borriello, 2023; Corbau et al., 2023; Ghosh et al., 2023). Studies indicate that the
32 presence of microplastics on beaches not only harms the physical beauty and tourist appeal but
33 also reflects issues in waste management and public perception of marine ecosystem health
34 (Amelia et al., 2021; Ghosh et al., 2023; Hartley et al., 2015; Oliveira et al., 2020). Furthermore,
35 this phenomenon not only reduces the attractiveness of these areas to visitant travelers but also
36 raises concerns regarding the health and well-being of both the local wildlife (Botero et al., 2021;
37 Costa et al., 2022; da Silva et al., 2022; Göktuğ, 2021).

38 From a physical perspective, MPs alter the composition and characteristics of beach
39 environments, with potential repercussions for coastal ecosystems and the organisms reliant on
40 these habitats for survival (Fries et al., 2013). MPs modify sediment porosity, thereby impacting
41 beach substrates' drainage and moisture retention capabilities. These changes in the physical
42 environment can influence temperature-dependent sex determination in certain species, such as
43 crustaceans and marine turtles (Carson et al., 2011; Nelms et al., 2016).

44 Chemically, MPs can absorb and concentrate organochlorine contaminants, which include
45 polychlorinated biphenyls (PCBs), dichlorodiphenyltrichloroethane (DDT), Polycyclic Aromatic
46 Hydrocarbons (PAHs) and MEHP (Mono-ethyl-hexylphthalate, degraded from Diethyl-hexyl-
47 phthalate or DEHP) (Brighty et al., 2015; Hartley et al., 2015; Ogata et al., 2009; Teuten et al.,
48 2009). Residual plastic from the action of UV rays and/or the process of mechanical abrasion
49 (Harris, 2020) begins to release greenhouse gases such as methane and ethylene (Royer et al.,
50 2018). These chemical compounds can concentrate and transport contaminants to marine biota

51 and, by extension, humans through the food chain (Rochman et al., 2013; Rochman et al., 2014;
52 Smith et al., 2018).

53 The Santos estuary, encompassing the city of Santos, its Port, and the industrial region of
54 Cubatão, represents a critical area for MP pollution, especially pellets, along the São Paulo coast
55 (Ferreira et al., 2021). Inadequate plastic waste management and failures in containment systems
56 are the leading causes of the entry of this pollutant into the environment, particularly during
57 production, transport, and transshipment processes in factories and port terminals (Geyer et al.,
58 2017; Jambeck et al., 2015).

59 The intense port activity, combined with high population density and industrial
60 concentration, makes this region a hub for the dispersion of MP (Jong et al., 2022). Ivar do Sul &
61 Costa (2014) pointed out that on Brazilian beaches, a high concentration of MP is correlated with
62 the intensity of port and industrial activities, especially in the Southeast region. The impacts caused
63 by this pollutant affect, among others, marine life due to the ingestion of these particles by marine
64 organisms, causing physical and chemical damage, reflecting the severity of the situation
65 (Rochman et al., 2013).

66 Through the combined analysis of geodetic, geomorphometric, and meteoceanographic
67 factors at a beach along the São Paulo coastline, Ferreira et al. (2021) demonstrated that factors
68 such as coastal currents and storm events can influence the deposition patterns of MP. Therefore,
69 identifying the most suitable zones for their accumulation and systematizing potential MP
70 accumulation areas are critical considerations (Avio et al., 2017; Hidalgo-Ruz et al., 2012a; Kim
71 et al., 2015; Van Cauwenberghe et al., 2015). This study aims to conduct a novel and extensive
72 evaluation of the correlations and interdependencies between various parameters, including the
73 abundance and characteristics of MP, such as their shape and polymer type, and morphometric
74 variables like elevation, slope, and orientation of beach facades. The focus is on identifying and
75 understanding the distribution of these deposits across approximately 880 kilometers of beaches
76 along the São Paulo coast in São Paulo, Brazil.

77 The primary research questions aim to identify critical accumulation points of MPs to better
78 direct remediation efforts. Understanding these aspects can help trace potential sources and
79 comprehend their behavior in the coastal and marine environment, linking geomorphological
80 aspects with pollution patterns. Finally, the study considers the implications of MP pollution for
81 marine life due to the ingestion of these materials and for the aesthetic and recreational experience
82 of beach visitors, emphasizing the importance of effective environmental monitoring and
83 remediation strategies.

84

85 2. Methods

86 To indicate locations susceptible to MP deposition (MP hotspots), the data collection and
87 analysis can be divided into three stages: 1) fieldwork – sediments sampling and beach
88 morphometric parameters (aspect, slope, and altitude) using altimetry from the Global Navigation
89 Satellite System (GNSS); 2) laboratory analysis – sieving (1 – 5 mm mesh) and μ -RAMAN
90 spectrometry for the confirmation of polymeric properties; 3) exploratory multivariate techniques
91 – analytical hierarchy process-gaussian (AHP-G) and correspondence analysis (CA) (Figure 1).

92

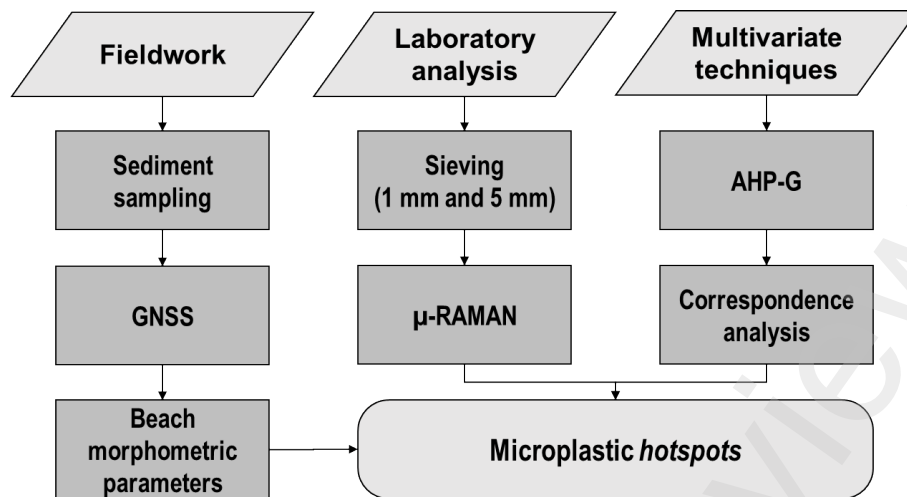


Figure 1. Flowchart summarizing the methods used in this research. GNSS: Global Navigation Satellite System; AHP-G: analytical hierarchy process-gaussian.

2.1. Study area

The almost 880 km coastline of São Paulo State in southeastern Brazil is segmented into six distinct compartments: (C1) Ilha do Cardoso to Serra do Itatins; (C2) Peruíbe to Praia Grande; (C3) Santos to Bertioga; (C4) Bertioga to Toque-Toque; (C5) Toque-Toque to Tabatinga; and (C6) Tabatinga to Picinguaba (Figure 2a), as outlined by Tessler et al. (2018). This coastline features diverse geomorphological characteristics such as beaches, rocky shores, sandbars, and mangroves, shaped by a combination of geological, geomorphological, climatic, and human factors (Ferreira et al., 2023).

A flatter topography characterizes the southern part of the coastline and includes critical ecological zones like the Juréia-Itatins and Itinguçu State Park (Suguio and Tessler, 1984; Tessler et al., 2018). Here, the Serra do Mar escarpment is situated further from the shore (10 km to 70 km), allowing for a wide coastal plain that features long, uninterrupted beaches and several islands (Souza, 2012; Tessler et al., 2018).

Moving northward from the central to the northernmost section, the Serra do Mar mountain range narrows the coastal plain. It reduces the size of hydrographic basins compared to the southern region. The northern coastline is more topographically diverse, with smaller, secluded beaches shaped into coves and bordered by pre-Cambrian rocky promontories found at locations like Itaguapé, Massaguaçu, and Praia Vermelha do Norte (Souza, 2012; Tessler et al., 2018). Significant urban centers such as Santos, which hosts the largest port in Latin America, are located in this region (Reid et al., 2022). The northern coastal area is characterized by sandy beaches interspersed with rocky outcrops and a rugged landscape, featuring the presence of the Serra do Mar and numerous nearby islands (Suguio et al., 1985).

The hydrodynamics along the Brazilian continental margin are governed primarily by the southward-flowing Brazil Current (BC) in deep waters and the Brazil Coastal Current (BCC), which travels from the south-southeast to the northeast along the continental shelf during spring and winter (Campos et al., 1995; De Souza and Robinson, 2004; Möller Jr et al., 2008). Predominant east-northeast winds create currents that run parallel to the northeast-southwest direction of the coastline. In winter, however, cold fronts influence the region, producing more intense south-southeast winds that generate stronger currents and waves from the southern quadrant (Andrade et al., 2019; Castro Filho et al., 1987; Ferreira et al., 2021; Harari et al., 2006; Pianca et al., 2010). Additionally, the urban development and coastal infrastructure significantly alter the coastal physiography and dynamics, potentially leading to erosion and progradation (Corrêa et al., 2021; Franzen et al., 2021).

2.2. Fieldwork samples and morphometric parameters

The field trips were conducted from April to September 2023, when the cold fronts produced waves of up to 4 m and approached the coast from the south and southeast quadrants. Favoring maximum sediment transport capacity, beach morphological changes, and microplastic deposition and/or remobilization (Ferreira et al., 2021). We opted for several varied beach profiles (32) that would proportionally cover the entire coast of São Paulo for each compartment, encompassing urban and rural beaches. Additionally, these locations were selected for their relatively easy accessibility by road, optimizing financial costs and time. Sediment samples and beach morphology parameters were obtained along beach profiles distributed across all six compartments of the São Paulo coastline, as shown in Table 1 and Figure 2a.

The locations of sediment collection along each beach profile were selected based on environmental factors influencing litter dynamics on sandy beaches (GESAMP, 2019), particularly water levels (strandline altitudes) pointed out by Ferreira et al. (2021). Approximately 1500 g of sediment were collected at each of the four water levels (Figure 2b): storm strandline (P1), spring high tide (P2), neap high tide (P3), and low tide (P4). The collected sediments were subsequently homogenized and separated into aliquots of 500 g to ensure consistency and repeatability of the sampling process, if necessary. This approach allowed for collecting samples from the top layer of sediment within a 1 m² area (Figure 2f) at each of the 128 sampling points, yielding 1026 items/pieces identified as large MP, between 1 – 5 mm (GESAMP, 2019).

Table 1 – List of beach profiles per coastal compartment.

Compartment	Profiles ID	Number of profiles
C1 Ilha do Cardoso – Serra do Itatins	IC-A, IC-B, IC-C, IC-D, IC-E, IC-F	6
C2 Peruíbe – Praia Grande	PER, ITA, MON, PG GZN, ITR, GZG, GUA-A, GUA-B, TMB,	4
C3 Santos – Bertioga	AST, PIT-A, PIT-B, ENS-A, ENS-B, MCS, PEB	14
C4 Bertioga – Toque-Toque	BET, GRT, BOR	3
C5 Toque-Toque – Tabatinga	TOG, SSB, CRG, MSS	4
C6 Tabatinga – Picinguaba	UBA, ITB, PIC	3

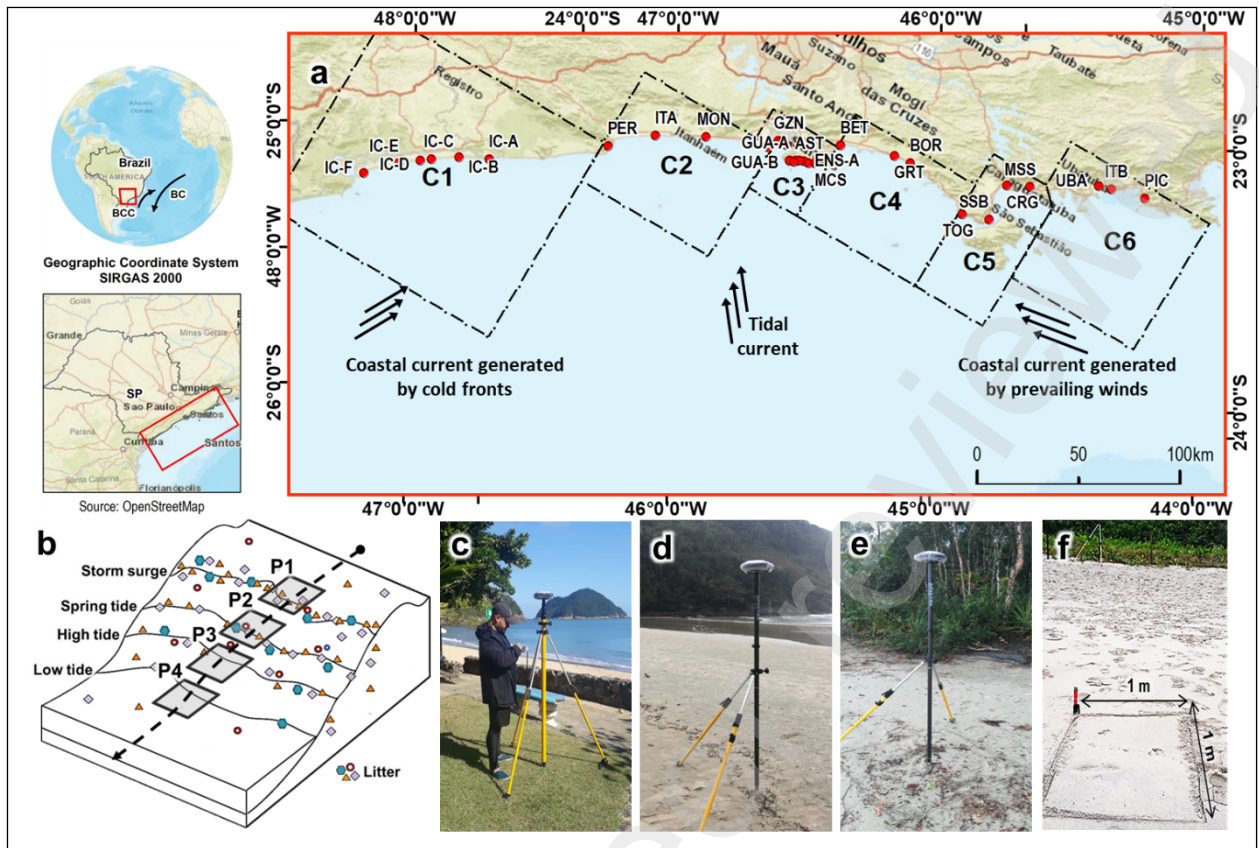


Figure 2 – (a) Sampling location distributed within the six compartments on the São Paulo coast. (BCC = Brazil Coastal Current, BC = Brazil Current), modified from Pianca et al. (2010); Tessler et al. (2018). (b) Sampling points by beach profile (P1, P2, P3, and P4), modified from GESAMP (2019); (c, d, and e) base and GNSS Rovers; (f) area (1 m²) of superficial sediment collection.

The morphometric parameters are divided into aspect, beach slope, and altitude. The first (aspect) is the beach face orientation determined by the direction of the beach transect relative to the geographic north as follows (Burrough et al., 1998): North – N (0° - 22.5°); Northeast – NE (22.5° - 67.5°); East – E (67.5° - 112.5°); Southeast – SE (112.5° - 157.5°); South – S (157.5° - 202.5°); Southwest – SW (202.5° - 247.5°); West – W (247.5° - 292.5°); Northwest – NW (292.5° - 337.5°); North – N (337.5° - 360°). The beach slope ($\tan\beta$) was derived from Eq. 2:

$$\tan\beta = \text{atan}(\text{VD}/\text{HD}) \quad (2)$$

VD and HD are the vertical and horizontal distances between sampling points P1 and P4 (Figure 2b). The slope can be used as a proxy of the beach morphodynamic stage (Bujan et al., 2019), and can be categorized into steep ($\tan\beta > 0.12$); intermediate ($0.05 < \tan\beta < 0.12$); and sloping ($\tan\beta < 0.05$) (Ferreira et al., 2023). The altitudes (H) of the sampling points were classified according to Ferreira et al. (2021), as: Very Low (VL; < 1.42 m); Low (L; $1.42 - 1.57$ m); Mean (M; $1.58 - 1.89$ m); High (H; $1.90 - 2.06$ m); and Very High (VH; > 2.06 m).

The altimetry of the sampling points (P1, P2, P3, and P4) was obtained using the GNSS, following the method described in Ferreira et al. (2021). Reference stations were established within less than 5 km of markers distributed along the beach, and positions were received from the nearest active stations of the Brazilian Network for Continuous Monitoring using the SIRGAS2000 coordinates system. Coordinates and altitudes of sampling points recorded by the mobile station were post-processed relative to the reference station (Monico, 2008; Monico et al., 2009) using the

180 Survey Office software. The orthometric altitude (H) relative to the mean sea level of the
181 Imbituba/SC datum of the Brazilian Geodetic System was obtained through Eq. 1 (Blitzkow et al.,
182 2016):

$$184 \quad H = h - N \quad (1)$$

185
186 Where h is the geometric altitude obtained with GNSS referenced to the SIRGAS2000
187 ellipsoid, and N is the geoidal height determined by the IBGE geoidal model - MAPGEO2015.
188

189 **2.3. Microplastic analysis**

190 **2.3.1. Polymeric characterization**

191 The MP was extracted by sieving the samples using 1 – 5 mm mesh. The retained MP were
192 visually separated from biological materials, such as shells, algae, and vegetation debris, and
193 subsequently identified, counted, and categorized according to shape (Löder and Gerdtts, 2015):
194 pellets (spherical or smooth), granular (foam), lines (fibers and filaments), and films (plastic film).

195 The polymeric characterization of MP was undertaken using μ -Raman spectroscopy
196 (McCreery, 2005), using lasers with wavelengths of 473 nm, 532 nm, 633 nm, and 785 nm and a
197 long-range 50x objective numerical aperture ($NA = 0.55$). First, the laser's power is calibrated to
198 obtain ideal spectra in the polymer identification region (around 1600 cm^{-1}) to prevent damage to
199 the materials. Subsequently, the analysis extends to the spectral region from 200 cm^{-1} to 3200 cm^{-1} ,
200 focusing on identifying hydrocarbons (Araujo et al., 2018; Ferraro, 2003; Smith and Dent, 2019).
201 Additionally, adjustments in integration time, number of accumulations, and slit diameter are made
202 to enhance the signal-to-noise ratio and avoid sensor saturation. A baseline is established for the
203 acquired spectra, with subsequent noise filtering via a computational routine in Matlab®. Finally,
204 the spectra are compared with the Knowitall® software database to identify polymer types.
205 Concurrently, images of the MP are captured by the Raman system microscope, complementing
206 the database.
207

208 **2.4. Unsupervised models**

209 Given the heterogeneous nature of the data, which includes both quantitative and
210 qualitative variables, we employed exploratory multivariate techniques such as the Analytical
211 Hierarchy Process-Gaussian (AHP-G) and Correspondence Analysis (CA). These algorithms were
212 chosen based on their simplicity and effectiveness for exploratory analyses. Specifically, the AHP-
213 G was utilized to analyze quantitative data and perform rankings, as it effectively represents these
214 types of data. Conversely, Correspondence Analysis was selected to examine qualitative variables,
215 also known as latent or categorical variables, which cannot be directly measured but can only be
216 categorized or counted (dos Santos et al., 2023; Fávero and Belfiore, 2017).

217 The AHP-G incorporates the Gaussian distribution to quantify and assess, through
218 distributions, uncertainties in evaluations and probabilistic decision-making while maintaining the
219 classic hierarchical structure of Saaty's AHP (2008), without arbitrary weighting (Dos Santos et
220 al., 2021; dos Santos et al., 2023). The result generates a ranking of MP abundance, subsequently
221 standardized (Eq. 3) and transformed into a Likert scale (Table 2), allowing an assessment of the
222 association between this ranking and beach morphometric parameters through CA.

223 The CA examines associations between variables of interest using the chi-square test (X^2 ;
224 $p\text{-value} < 0.05$). In it, the Adjusted Standardized Residuals (ASR) check for dependence
225 relationships between each variable based on the reference critical value ($+1.96 \leq$) of the standard
226 normal curve for a 5% significance level. Thus, if the value of the ASR in a cell is greater than or
227 equal to 1.96, it is interpreted that significant dependence relationships exist (Fávero and Belfiore,
228 2017; Haberman, 1978; Johnson and Wichern, 1992). All statistical analyses were performed using
229 Python in Anaconda/Spyder software.

230
231
232
233

$$\text{Standardization} = \frac{(\text{observed value}) - (\text{minimum value})}{(\text{maximum value}) - (\text{minimum value})} \quad (3)$$

Table 2 – Standardized qualitative data based on the total count of polymers.

Ranking	Qualitative data
0.80 – 1.00	Very High (VH)
0.60 – 0.79	High (H)
0.40 – 0.59	Moderate (M)
0.20 – 0.39	Low (L)
0.00 – 0.19	Very Low (VL)

234

3. Results

235
236

3.1. Geographic distribution of microplastic

237
238
239
240
241
242
243

The 34 transects perpendicular to the coastline had an average width of 37.57 m, with minimum and maximum values of 5.52 m and 182.48 m, respectively. The beach faces had an average direction of 158° (SE), with values varying from 43° (N) to 259° (W). The slope of these faces was predominantly intermediate. In Table 3, it is possible to observe that fragments, Foams, and Pellets appeared in more significant quantities when compared to Fibers and Films. The same table also shows that the highest proportions of this material are found mainly in P1 (highest points of the beach profile), gradually decreasing to P4 (close to the waterline) (Table 3).

244
245
246
247
248
249
250

Most of the 1,026 MP items found consisted of fragments (42%) and foams (35%), with pellets, fibers, and films accounting for 20%, 3%, and 0.3%, respectively. Figure 3 shows the distribution of the standardized MP ranking across the study area. Low (L) and very low (VL) MP concentrations were found on beaches across all coastal compartments. In contrast, very high (VH) concentrations were predominantly found on beaches located in compartments C2 and C3 (PIT-B and ITA), with high (H) and moderate (M) concentrations identified in C4 and C1 (BOR and IC-D), respectively.

251
252
253

Table 3 – Absolute and percentage values of items sampled collectively for each corresponding position across all collection points.

Point	Pellet	Fragment	Fiber	Foam	Film	Total	%
P1	70	105	9	167	0	351	34
P2	59	133	7	69	2	270	26
P3	51	86	3	80	0	220	22
P4	26	103	7	48	1	185	18

254

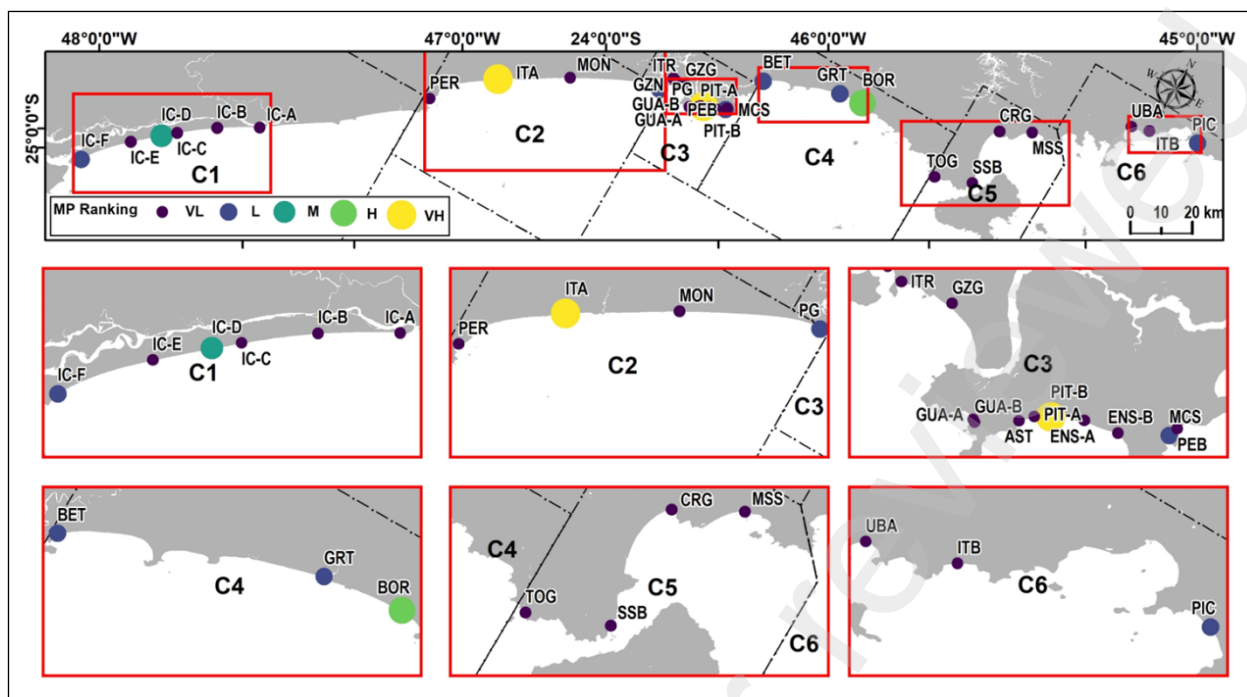
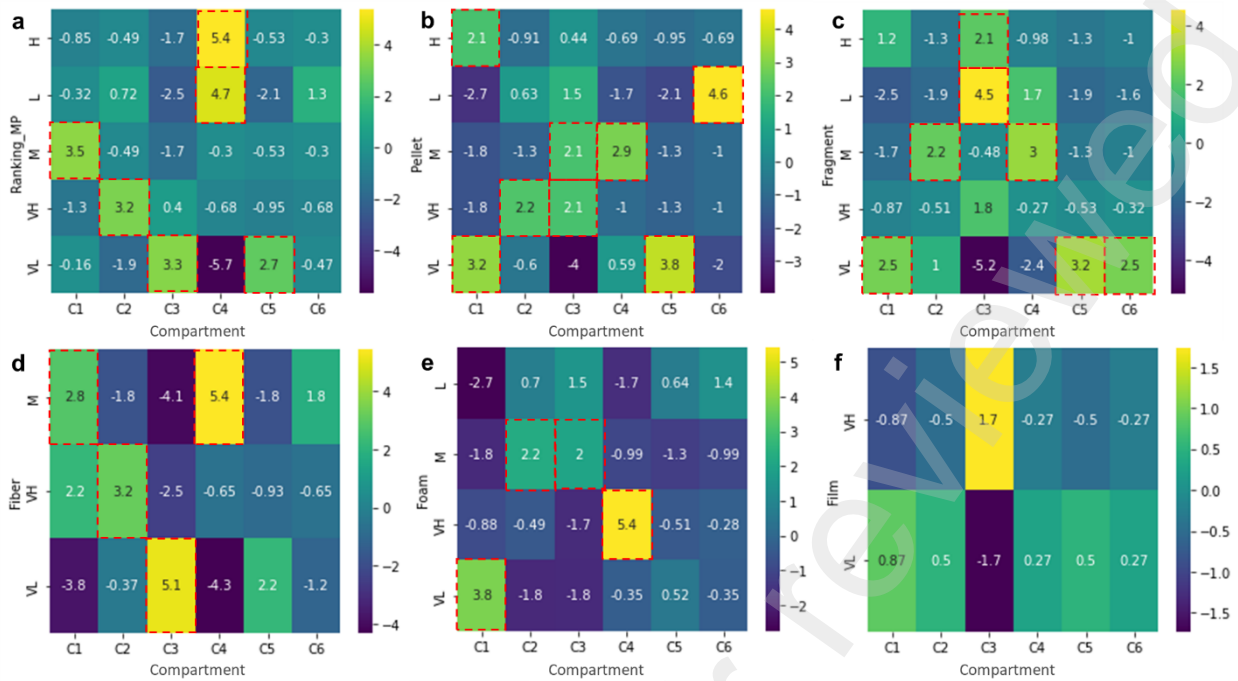


Figure 3 – The AHP-G method generated an MP ranking for the entire coast of São Paulo, emphasizing compartments C1, C2, C3, C4, C5, and C6. The map features circles of varying sizes that represent Very High (VH), High (H), Moderate (M), Low (L), and Very Low (VL), respectively.

The X^2 statistical test indicated statistically significant associations ($p < 0.05$) between the presence of all types of MP and the specific compartments in which they were found, except for films ($p = 0.6885$). The CA identified a clear dependency relationship ($ASR \geq 1.96$) between high (H) and very high (VH) MP concentrations and compartments C2 and C4, respectively. On the other hand, moderate (M), low (L), and very low (VL) concentrations were observed in compartments C1, C4, C3, and C5, in this order (Figure 4a). No significant relationship was found between MP concentrations and C6.

The concentration of pellets exhibited significant variations between compartments. Very high (VH) concentrations of pellets were significantly associated with beaches in C2 and C3 (Figure 4b). Significant associations were found between high (H) and very low (VL) concentrations of pellets in C1 beaches, with VL also found in C5. Moderate (M) concentrations were associated with beaches in C3 and C4, while low concentrations were significantly associated only with beaches in C6 (Figure 4b). Considering fragments, no significant association was found for VH concentrations, while H concentrations showed a significant relationship only with beaches in C3 (Figure 4c). Moderate concentration of fragments was significantly related to beaches in C2 and C4, with low concentrations associated with C3. Very low (VL) concentrations were significantly related to C1, C5, and C6. The presence of fibers showed no significant relationships with beaches in C5 and C6. At the same time, VH and VL concentrations were associated with beaches in C2 and C3, respectively, and moderate (M) concentrations with beaches in C1 and C4 (Figure 4d). Similar to fibers, the presence of foam showed no significant relationships with C5 and C6. Significant associations were found between VH foam concentration in C4, M in C2 and C3, and VL in C1 (Figure 4e). Films did not display significant dependency relationships with any compartment, although C3 exhibited the highest ARS values (Figure 4f).

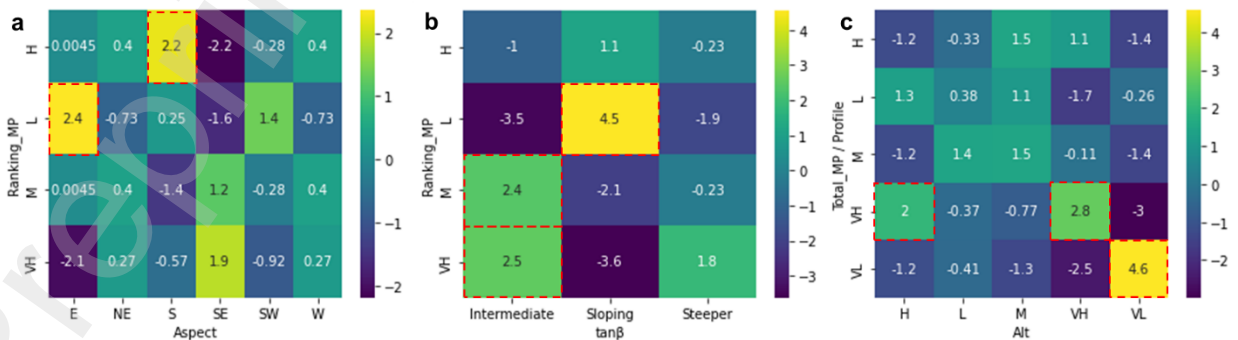


285
 286 Figure 4 – Matrices showing the Adjusted Standardized Residual (ASR) values between the
 287 concentration rankings for MP (a), pellets (b), fragments (c), fibers (d), foam (e), and film (f) for
 288 each compartment (C1, C2, C3, C4, C5, and C6). Dashed red contours indicate variables
 289 exhibiting significant dependency relationships (ASR ≥ 1.96).
 290

291 **3.2. Associations between morphometric variables and microplastics**

292 The X^2 test showed statistically significant associations between beach slope ($\tan\beta$
 293 $p=2.2239E-07$), aspect ($p=1.1805E-06$), altitude ($p=0.0016$), and MP concentrations. Dependency
 294 relationships were identified between high MP concentrations and a southerly beach aspect (the
 295 slope faces the S quadrant). In contrast, low MP concentrations (L) were associated with an easterly
 296 beach aspect (Figure 5a). Very high and moderate MP concentrations showed a significant
 297 relationship with beach slopes classified as intermediate ($0.05 < \tan\beta < 0.12$), with low
 298 concentrations associated with gentler beach slopes ($\tan\beta < 0.05$), as illustrated in Figure 5b.

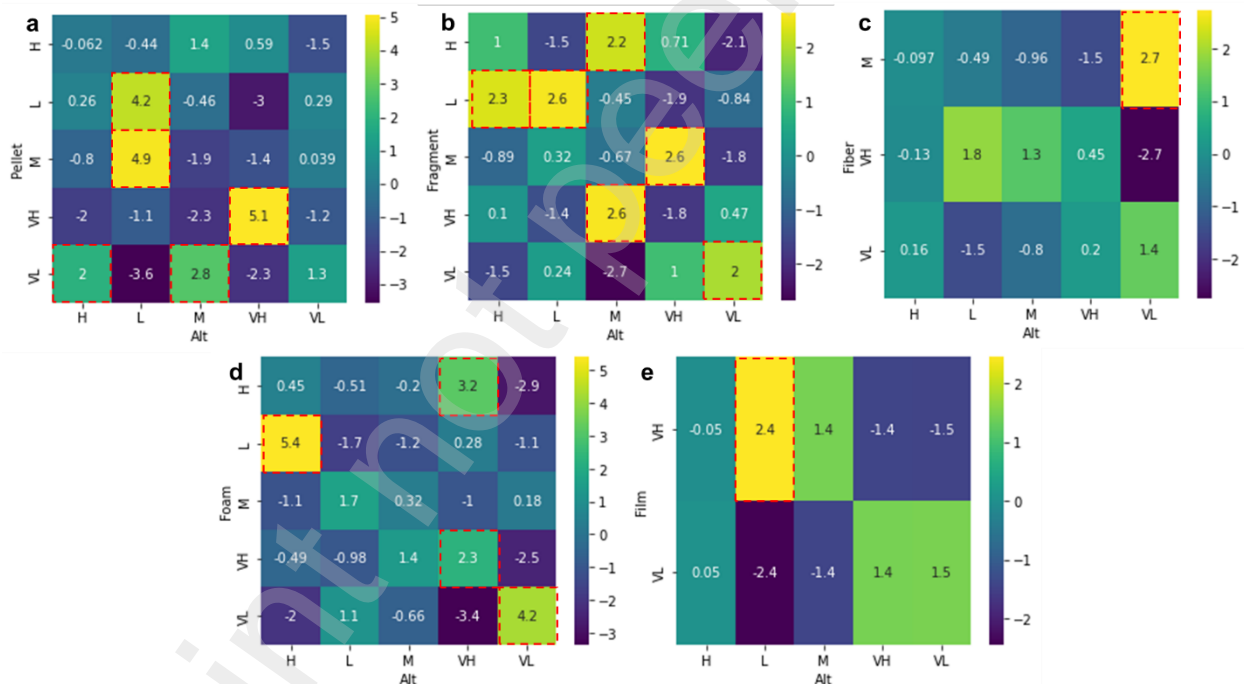
299 The analysis of ASR values indicated that very high MP counts along the beach profile are
 300 significantly related to high and very high altitudes (Figure 5c), reflecting strandlines along the
 301 upper parts of the beach profile (2.06 m to 2.62 m above mean sea level). Conversely, very low
 302 MP concentrations were associated with very low altitudes (<1.90 m), suggesting strandlines along
 303 the lower part of the beach profile.
 304



305
 306 Figure 5 – Matrices showing the Adjusted Standardized Residual (ASR) values between MP
 307 rankings and the orientation of the beach face (Aspect) (a); beach slope ($\tan\beta$) (b), the total MP

308 count per profile and the altitude (Alt) (c). Dashed red contours indicate significant relationships
 309 (ASR ≥ 1.96).
 310

311 Results from the X^2 tests reveal that different MP types are more likely to be found at
 312 specific beach elevations, with significant associations ($p < 0.05$) found between altitude levels
 313 and pellets ($p=1.6604E-10$), fragments ($p=0.0003$), fibers ($p=0.03677$), foam ($p=5.69E-08$), and
 314 film ($p=0.04353$). Very high pellet concentrations were associated with very high altitudes (the
 315 upper beach), while low and moderate concentrations were significantly more prevalent in low
 316 and moderate altitudes (Figure 6a). High and very high concentrations for fragments were
 317 significantly associated with moderate altitudes (Figure 6b), with concentrations reducing in
 318 higher and lower beach elevations. Concentrations of fragments were very low at the lowest beach
 319 elevations, low at both high and low beach levels, and moderate at high and very high altitudes
 320 (Figure 6b). The accumulation of fibers showed a significant relationship only between moderate
 321 concentrations and very low altitudes (Figure 6c). Similar to fragments, very low concentrations
 322 of foam were significantly associated with very low altitudes and low concentrations were
 323 associated with high altitudes (Figure 6d). However, high and very high foam concentrations were
 324 found at the highest parts of the beach rather than at moderate altitudes as shown for fragments.
 325 Finally, very high film concentrations were associated with low altitudes, the only significant
 326 relationship found between this type of MP and altitude (Figure 6e).
 327



328
 329 Figure 6 –Matrices of the Adjusted Standardized Residual (ASR) values between altitude (Alt)
 330 and the total count of pellets (a), fragments (b), fibers (c), foams (d), and films (e) per profile.
 331 Dashed red contours indicate significant relationships (ASR ≥ 1.96).
 332

333 3.3. μ -Raman analysis

334 At the sites where the highest MP concentrations were observed (beach profiles IC-D in
 335 C1, ITA in C2, PIT-B in C3, and BOR in C4, Figure 3), the μ -Raman analyses indicated that most
 336 pellets found on the upper beach were primarily polymers derived from high (HDPE) and low-
 337 density Polyethylenes (LDPE), along with other copolymers (Table 4). They were typically found
 338 in the form of small spherical or cylindrical granules, with HDPE exhibiting significant Raman
 339 peaks around 1130 cm^{-1} , 1295 cm^{-1} , and 1460 cm^{-1} , and a density range between 0.941 and 0.965

340 g/cm³. LDPE showed Raman peaks similar to those of HDPE, maintaining the same characteristic
 341 peaks at 1130 cm⁻¹, 1295 cm⁻¹, and 1460 cm⁻¹, but with subtle differences in the spectral profile
 342 and a lower density range (0.910 to 0.940 g/cm³).

343 The fragments and the fibers predominantly found at moderate altitudes in the beach profile
 344 exhibited the greatest diversity of polymeric material. As they are derived from already
 345 industrialized products, these are commonly found in the form of polymers such as high and low-
 346 density Polyethylenes (HDPE and LDPE, respectively), identical to the pellets in Figures 7a and
 347 b, as well as Polypropylene (PP), and other copolymers including Ethylene-Polypropylene,
 348 Poly(Ethylene-co-Vinyl Acetate), Poly(Propylene-Ethylene-Acrylic Acids), and High Ethylene
 349 Random Copolymer (RCP) (Table 1). PP is identified in the Raman spectrum by its distinct peaks
 350 at 841 cm⁻¹, 973 cm⁻¹, and 1160 cm⁻¹, with a density ranging between 0.855 and 0.946 g/cm³.

351 Similarly to the fragments, foams also stood out for the diversity of their compounds. These
 352 polymers were predominantly identified and classified as Polystyrene, Polyurethane, and
 353 Styrene/Allyl Alcohol Copolymers with Low Molecular Weight (Table 2). Meanwhile, films
 354 primarily featured materials derived from polyethylene (Table 2). Styrene, a base monomer for
 355 polystyrene production, exhibits peaks in the Raman spectrum at 1000 cm⁻¹, 1030 cm⁻¹, and 1600
 356 cm⁻¹. The density of polystyrene, a styrene derivative, is approximately 0.91 g/cm³.

358 Table 4 – Main Polymers Identified by μ -Raman Spectrometry at different beach elevations (IC-
 359 D, ITA, PIT-B, and BOR).

Pellet	Fragment	Fiber	Foam	Film
High and Low Density Polyethylene	High and Low Density Polyethylene	High and Low Density Polyethylene	Styrene	Polyethylene
Poly(Ethylene), p-(Ethylene-co-Acrylic-Acid)	Polypropylene		Polystyrene	
	Ethylene-Polypropylene		Polyurethane	
	Poly(Ethylene-co-Vinyl Acetate)		Styrene/Allyl Alcohol Copolymer Low Molecular Weight	
	Poly(Propylene-Ethylene-Acrylic Acids)			

360
 361 **4. Discussion**
 362 **4.1. Factors responsible for the MP distribution and accumulation along the coast**
 363 The MP Ranking observed a distribution starting from the Santos Estuary and Mar Pequeno
 364 (São Vicente), initially depositing on beaches near these channels (e.g., sectors C3 and C2) and
 365 progressively accumulating as it moves toward the SSW, the same direction as the predominant
 366 coastal current in the region (NE-SW) (Tessler et al., 2018) on beaches such as Itanhaém (ITA)
 367 and those located on Ilha Comprida (IC-D), in sectors C2 and C1 of Figure 3, respectively.
 368 Conversely, beaches in sectors C4, C5, and C6 showed the lowest values in the Ranking. This
 369 suggests that beaches near Santos Bay are the first to be impacted due to their proximity to the
 370 primary sources of this pollutant, resulting from cities with higher population densities like Santos
 371 and São Vicente, in addition to the Port of Santos and the petrochemical industries in Cubatão. The
 372 latter two are responsible for the reception and processing of this material (Balthazar-Silva et al.,
 373 2020; Ferreira et al., 2021; Turra et al., 2014).

374 The analysis of the results on the distribution of MP across different compartments of the
375 São Paulo coast provides a comprehensive overview of the environmental impact of this pollutant.
376 The applications of AHP-G, the χ^2 test, and CA have provided a robust statistical understanding of
377 the distribution of these materials (Ferreira et al., 2023; Pereira et al., 2023; Santos et al., 2021).

378 Regarding different types of MP, the lack of a significant relationship for films suggests a
379 distinct distribution dynamic or emission sources compared to other types of MP. This observation
380 aligns with research indicating variations in sources and their environmental persistence (Tiwari
381 et al., 2023).

382 The analysis of pellets and fragments shows significant dependence on specific
383 compartments, indicating potential point sources of pollution or specific transport and deposition
384 processes for these materials (Barnes et al., 2009; Lebreton et al., 2017). The high concentration
385 of these materials in specific compartments (C3 and C2) underscores the need for more competent
386 handling, transport, and manufacturing management (Tian et al., 2023). For fibers, the observed
387 distribution suggests wide dispersion across different compartments, aligning with studies
388 indicating their release from various sources, including the wear of synthetic fabrics and fishing
389 nets (Oliveira et al., 2023; Zhang et al., 2022).

390 The results for foam are exciting, given the high dependency relation with compartment
391 C4. This observation may be attributed to this material's specific characteristics or sources near
392 this compartment. On beaches, foam is commonly associated with waste from fishing materials or
393 insulated containers for storing beverages and/or food, typically used by merchants and/or
394 beachgoers (Chen et al., 2022; Zeng, 2023; Ziani et al., 2023).

395 The analysis of results regarding morphometric variables and their relationship with MP
396 concentrations on beaches provides a relevant understanding of the distribution of this pollutant
397 on the São Paulo coast and in the coastal environment. The χ^2 test and the analysis of RPA reveal
398 statistically significant associations between the physical characteristics of the beaches and the
399 presence of MP, aligning with previous studies that highlight the influence of geomorphological
400 factors on the accumulation of marine debris (Ferreira et al., 2021; Hidalgo-Ruz and Thiel, 2013).

401 The relationship between the beach slope ($\tan\beta$) and the concentration of MP suggests that
402 beaches with intermediate slope profiles are more prone to accumulate higher concentrations of
403 MP, in general. This may be due to sediment and debris transport and deposition dynamics on
404 these profiles (Andrady, 2011; Ferreira et al., 2021). Beaches with a dissipative trend ($\tan\beta < 0.05$)
405 show lower concentrations. The flatter and lower profiles favor beach washing during high tides
406 and, consequently, the fluctuation of MP back into the coastal current (Cooper and McLaughlin,
407 1998; Ferreira et al., 2021). The orientation of the beaches (Aspect) also shows a significant
408 relationship with the concentration of MP (Vito et al., 2022). Beaches facing the South quadrant
409 exhibit higher concentrations in the same direction as the higher energy storm waves (Ferreira et
410 al., 2021; Young and Elliott, 2018) come from this direction. According to Ferreira et al.
411 (2023) With this orientation, beaches on the São Paulo coast naturally accumulate sediments and
412 marine litter.

413 Regarding altitude, the observed association between higher altitudes and higher MP
414 concentrations can be attributed to the deposition of debris brought by high tide processes
415 combined with storm events, which deposit material in higher areas of the beach (Álvarez-
416 Hernández et al., 2019; Ferreira et al., 2021; Lavers and Bond, 2017; Schmuck et al., 2017; Young
417 and Elliott, 2018). The distribution of pellets, fragments, fibers, foams, and films about altitude
418 reinforces the idea that different types of MP have distinct distribution dynamics, possibly
419 influenced by their physical characteristics and sources of origin (Hidalgo-Ruz et al., 2012b).

420 This way, based on the aspects raised (Aspect, $\tan\beta$, and Altitude), it is possible to state
421 that the locations with greater susceptibility to MP accumulation or potential hotspots depend on
422 intermediate beach profiles facing the South quadrant and locations with excellent coastline
423 stability and/or accretion. This is due to the $\sim 90^\circ$ angle between storm waves formed by cold fronts

424 coming from the same quadrant, resulting in the near cessation of sediment transport on these
425 beaches, favoring the accumulation of sediments and anthropogenic debris, including MP (Ferreira
426 et al., 2023, 2021; Harris, 2020; Jong et al., 2022; Laurino et al., 2023; Stein and Siegle, 2019).
427 This is because relative stability at some beaches can favor such deposition (Veerasingam et al.,
428 2020), as seen in those associated with slow accretion processes, such as sandy spits and areas
429 protected by tombolos, respectively, in compartments C1 and C3 (Ferreira et al., 2023; Mahiques
430 et al., 2016; Mascagni et al., 2018; Silva et al., 2021).

431 Due to the configuration of the São Paulo coastline (SW-NE), beaches facing SE are more
432 susceptible to erosive processes, as the acute angle ($\sim 45^\circ$) of incidence of storm waves (South) can
433 reach up to 4.0 m (Andrade et al., 2019; Ferreira et al., 2023, 2021; Stein and Siegle, 2020, 2019)
434 during the austral autumn and winter (April to September), favoring maximum sediment transport
435 capacity (Lavenère-Wanderley and Siegle, 2019; Pianca et al., 2010; Sousa et al., 2013; Stein and
436 Siegle, 2020, 2019). On erosive beaches, sand removal can expose buried layers containing MP,
437 increasing their availability to the marine environment (Ranjani et al., 2022; Sun et al., 2021; Wang
438 et al., 2021).

439 In this context, the seasonal incidence of storms and extreme events (increasingly frequent)
440 on the São Paulo coast (Gramcianinov et al., 2023; Nunes et al., 2018) may alter the MP dynamics.
441 During storms, the resuspension and redistribution of sediments can increase the mobility of this
442 pollutant (Cheung and Not, 2023). Harris et al. (2021) and Lebreton et al. (2017) emphasize that
443 estuaries are significant vectors for transporting MP to the sea, influenced by urbanization and
444 human activities. Thus, areas near river mouths and estuarine channels, such as those in Santos,
445 São Vicente, and Bertioga, are critical points for the entry of MP into the ocean.

446
447 **4.2. Polymer Diversity and microplastic accumulation**

448 The diversity of polymers found in fragments and fibers, including PE, PP, and various
449 copolymers, suggests a variety of pollution sources. These materials are often derived from already
450 industrialized and discarded products, reflecting the widespread use of plastics in modern society
451 and the inadequacy of waste management systems (Gao et al., 2022; Geyer et al., 2017). The
452 identified foams and films, mainly composed of styrene and other polymers such as polystyrene
453 and polyurethane, are consistent with literature highlighting the presence of these materials in
454 marine environments. The former (styrene and polystyrene) are commonly used in packaging and
455 thermal insulation applications due to their lightness and resistance. Polyethylene, widely used as
456 the primary material in the manufacture of plastic bags and packaging, represents one of the most
457 significant sources of MP pollution in the marine environment (Gao et al., 2023; Gunawan et al.,
458 2022; Katsara et al., 2022).

459 The accumulation of pellets in the higher portions of beach profiles is a phenomenon that
460 can be attributed to a combination of physical and geomorphological factors (Ferreira et al., 2021).
461 These pellets' spherical or cylindrical shape and relatively low density (0.910 and 0.965 g/cm³)
462 play a crucial role in their deposition and distribution on beaches. This enhances the transport of
463 these microplastics by ocean currents and, specifically, their mobilization by high-energy waves
464 and winds. When high-energy waves strike the beaches, particularly during high tides and storm
465 events, these microplastics are driven to the upper sections of the beach profiles. Moreover, the
466 spherical or cylindrical shape of the pellets reduces friction with the sand and other beach
467 materials, facilitating wind transport through rolling and/or saltation. Once in the higher areas of
468 the beach profile, these MP tend to be retained due to the decreased energy of these factors (waves,
469 winds, and tides), where they end up depositing and accumulating (Alvarez-Zeferino et al., 2020;
470 Ferreira et al., 2021; Ryan et al., 2009).

471 In contrast to pellets, fragments, and fibers often exhibit faceted or irregular shapes,
472 influencing their transport dynamics and deposition on beaches. These irregular shapes increase
473 resistance to movement in this environment, limiting their ability to be transported to higher beach

474 areas, especially under the influence of less intense winds and waves (Oliveira et al., 2023;
475 Lefebvre et al., 2023; Zhang et al., 2022). Furthermore, the density of these MP, generally higher
476 than that of pellets, also contributes to their accumulation in the mid-regions (P2 and P3) of the
477 beach profile. Fragments and fibers tend to settle where wave and current energy diminish, but it
478 is still sufficient to mobilize them. This intermediate zone of the beach profile typically
479 corresponds to a balance between areas reached by high tides and the extent of significant aeolian
480 transport (Andrady, 2011; Ferreira et al., 2021; Jambeck et al., 2015).

481 The accumulation of expanded foams and plastic films in higher concentrations in the lower
482 parts of beach profiles (P4, primarily, and P3) can be attributed to specific characteristics of these
483 materials and the environmental dynamics of beaches. Foam, commonly composed of polystyrene
484 and polyurethane, has a cellular structure that endows low-density and high buoyancy (Auta et al.,
485 2017; Gao et al., 2023). This low density allows foam easily transported by water, particularly by
486 waves. However, its voluminous structure and lightness contribute to these materials being
487 deposited in the lower parts of beach profiles, where wave energy is insufficient to carry them to
488 higher areas. In contrast, plastic films are generally thin and flexible, facilitating their movement
489 by wind and wave action. Nevertheless, their flat shape and larger surface area relative to weight
490 mean they are easily trapped in the lower beach areas (P4), where wind and wave energy is lower.
491 Additionally, plastic films can become entangled with natural debris or adhere to moist sand,
492 reducing mobility (Andrady, 2011; Barnes et al., 2009; Browne et al., 2011; Martin et al., 2017;
493 Rochman et al., 2013; Thompson et al., 2004).

494

495 **5. Conclusions, limitations, and future perspectives**

496 This study provided a comprehensive examination of the distribution of various types of
497 MP (categories: pellet, fragment, fiber, foam, and film) along the São Paulo coastline, considering
498 morphometric characteristics (beach face orientation - aspect; slope - tan β ; and altitude) and
499 meteo-oceanographic conditions. It revealed complex and significant patterns in the dispersion and
500 accumulation of MPs. Robust statistical analyses, including AHP-G, the X² test, and
501 Correspondence Analysis (CA), identified statistically significant associations between MP
502 presence and specific geographic compartments and morphometric variables of the beaches.
503 Notably, the highest concentrations of MPs were found predominantly on beaches in
504 compartments C3 and C2, suggesting a direct influence of proximity to urban and industrial
505 sources, such as the Santos Estuary and Mar Pequeno. Different types of MPs, including pellets,
506 fragments, fibers, and foams, exhibited distinct patterns of dependency on these compartments,
507 reflecting potential differences in emission sources, transport, and deposition processes. The
508 relationship between environmental characteristics MP accumulation dynamics was
509 comprehensively understood. Higher altitudes were associated with elevated MP concentrations,
510 indicating a significant role of high tide processes and storm surges in depositing debris in higher
511 beach areas.

512 μ -Raman spectroscopy revealed a predominance of polymers such as polyethylene (PE) in
513 high and low-density forms, polypropylene (PP), and styrene, underscoring the significant
514 contribution of industrialized and consumer products to MP pollution. The study identified
515 susceptible locations for MP accumulation (hotspots) along the coastline, using remote sensing
516 data and morphometric analyses. These hotspots were often associated with intermediate beach
517 profiles facing the Southern quadrant and areas with greater stability or shoreline accretion, where
518 aggradation processes favored the accumulation of anthropogenic debris, including MPs.

519 The findings highlight the complexity of MP dynamics in the coastal environment and
520 emphasize the importance of considering both the physical characteristics of beaches and local
521 human activities to understand and manage this type of pollution. The variability in MP types and
522 their relationships with different beach environments points to the need for differentiated

523 management approaches tailored to the specific characteristics of each coastal compartment and
524 pollutant type.

525 However, the study has some limitations. The samples were collected only once over six
526 months during the cold front period, not accounting for temporal variability due to seasonal
527 changes, sediment composition, sedimentary processes, or human activities, which could provide
528 new interpretations of the data. Additionally, the sampling depth limited to the top 4-5 centimeters
529 of a 1 m² area, potentially not reflecting the entire topographic profile of the beach and the more
530 stable, deeper sediment layers. The absence of detailed information on human activities,
531 urbanization, and industrialization also limits the understanding of the direct impact on MP
532 distribution.

533 Future studies linking these results with data derived from orbital remote sensing could
534 generate models capable of predicting and synoptically expanding all these aspects. Understanding
535 these distribution patterns is crucial for developing effective monitoring and environmental
536 remediation strategies along the São Paulo coast and other similar coastal regions. This contributes
537 to achieving Sustainable Development Goal 14 (Life Below Water), specifically targeting goal
538 14.1 — to prevent and significantly reduce marine pollution, particularly from land-based
539 activities, including marine debris (indicator 14.1.1 — density of plastic debris) by 2025 — and
540 goal 14.a, which seeks to enhance scientific knowledge, develop research capacities, and transfer
541 technology to improve ocean health (<https://sdgs.un.org/goals/goal14>).

542

543 6. Acknowledgment

544 The authors thank the Oceanographic Institute of the University of São Paulo, the Nuclear
545 and Energy Research Institute, the Institute of Energy and Environment of the University of São
546 Paulo, the Institute of Geosciences of the State University of Campinas and the São Paulo State
547 Technological College of Jahu, the São Paulo Research Foundation (FAPESP grant #2020/12050-
548 6), N.U.W. (FAPESP grant #2021/-4334-7), E.S. (#308229/2022-3), C.H.G. (#311209/2021-1)
549 and R.C.O. (#306931/2022-2) are National Council for Scientific and Technological Development
550 (CNPq) research fellows. Acknowledgments are extended to the Editor-in-Chief, Associate Editor,
551 and anonymous reviewers.

552

553 7. Data Availability Statement

- 554 • Data table < <https://doi.org/10.5281/zenodo.12193104>>
- 555 • Raman spectroscopy analysis < <https://doi.org/10.5281/zenodo.12193201>>

556

557 8. References

- 558 Álvarez-Hernández, C., Cairós, C., López-Darias, J., Mazzetti, E., Hernández-Sánchez, C., González-
559 Sálamo, J., Hernández-Borges, J., 2019. Microplastic debris in beaches of Tenerife (Canary Islands,
560 Spain). *Mar Pollut Bull* 146, 26–32.
- 561 Alvarez-Zeferino, J.C., Ojeda-Benítez, S., Cruz-Salas, A.A., Martínez-Salvador, C., Vázquez Morillas, A.,
562 2020. Dataset of quantification and classification of microplastics in Mexican sandy beaches. *Data*
563 *Brief* 33, 106473.
- 564 Amelia, T.S.M., Khalik, W.M.A.W.M., Ong, M.C., Shao, Y.T., Pan, H.-J., Bhubalan, K., 2021. Marine
565 microplastics as vectors of major ocean pollutants and its hazards to the marine ecosystem and
566 humans. *Prog Earth Planet Sci* 8, 1–26.
- 567 Andrade, T.S. de, Sousa, P.H.G. de O., Siegle, E., 2019. Vulnerability to beach erosion based on a coastal
568 processes approach. *Applied Geography* 102, 12–19.
- 569 Andrady, A.L., 2011. Microplastics in the marine environment. *Mar Pollut Bull* 62, 1596–1605.
- 570 Araujo, C.F., Nolasco, M.M., Ribeiro, A.M.P., Ribeiro-Claro, P.J.A., 2018. Identification of microplastics
571 using Raman spectroscopy: Latest developments and future prospects. *Water Res* 142, 426–440.
- 572 Auta, H.S., Emenike, C.U., Fauziah, S.H., 2017. Distribution and importance of microplastics in the marine
573 environment: a review of the sources, fate, effects, and potential solutions. *Environ Int* 102, 165–176.

574 Avio, C.G., Gorbi, S., Regoli, F., 2017. Plastics and microplastics in the oceans: From emerging pollutants to emerged threat. *Mar Environ Res* 128, 2–11.

575

576 Balthazar-Silva, D., Turra, A., Moreira, F.T., Camargo, R.M., Oliveira, A.L., Barbosa, L., Gorman, D.,

577 2020. Rainfall and Tidal Cycle Regulate Seasonal Inputs of Microplastic Pellets to Sandy Beaches.

578 *Front Environ Sci* 8.

579 Barnes, D.K.A., Galgani, F., Thompson, R.C., Barlaz, M., 2009. Accumulation and fragmentation of plastic

580 debris in global environments. *Philosophical Transactions of the Royal Society B: Biological Sciences*

581 364, 1985–1998.

582 Blitzkow, D., de Matos, A.C.O.C., Xavier, E.M.L., Fortes, L.P.S., 2016. MAPGEO2015: O novo modelo

583 de ondulação geoidal do brasil. *Revista Brasileira de Cartografia* 1873–1884.

584 Borriello, A., 2023. Preferences for microplastic marine pollution management strategies: An analysis of

585 barriers and enablers for more sustainable choices. *J Environ Manage* 344, 118382.

586 Botero, C.M., Tamayo, D., Zielinski, S., Anfuso, G., 2021. Qualitative and quantitative beach cleanliness

587 assessment to support marine litter management in tropical destinations. *Water (Basel)* 13, 3455.

588 Brighty, G.C., Jones, D., Ruxton, J., 2015. High-Level Science Review for ‘ A Plastic Oceans ’ Film.

589 Browne, M.A., Crump, P., Niven, S.J., Teuten, E., Tonkin, A., Galloway, T., Thompson, R., 2011.

590 Accumulation of microplastic on shorelines worldwide: sources and sinks. *Environ Sci Technol* 45,

591 9175–9179.

592 Bujan, N., Cox, R., Masselink, G., 2019. From fine sand to boulders: Examining the relationship between

593 beach-face slope and sediment size. *Mar Geol* 417, 106012.

594 Campos, E., Miller, J., Müller, T., Peterson, R., 1995. Physical Oceanography of the Southwest Atlantic

595 Ocean. *Oceanography* 8, 87–91.

596 Carson, H.S., Colbert, S.L., Kaylor, M.J., McDermid, K.J., 2011. Small plastic debris changes water

597 movement and heat transfer through beach sediments. *Mar Pollut Bull* 62, 1708–1713.

598 Castro Filho, B.M. de, Miranda, L.B. de, Miyao, S.Y., 1987. Condições hidrográficas na plataforma

599 continental ao largo de Ubatuba: variações sazonais e em média escala. *Boletim do Instituto*

600 *Oceanográfico* 35, 135–151.

601 Chen, S., Lin, D., Gao, G., Guan, J., Belver, C., Bedia, J., 2022. Sources, Aging, and Management of Coastal

602 Plastics in Shanghai. *Water Air Soil Pollut* 233, 437.

603 Cheung, C.K.H., Not, C., 2023. Impacts of extreme weather events on microplastic distribution in coastal

604 environments. *Science of The Total Environment* 904, 166723.

605 Cooper, J.A.G., McLaughlin, S., 1998. Contemporary multidisciplinary approaches to coastal classification

606 and environmental risk analysis. *J Coast Res* 512–524.

607 Corbau, C., Lazarou, A., Buoninsegni, J., Olivo, E., Gazale, V., Nardin, W., Simeoni, U., Carboni, D., 2023.

608 Linking marine litter accumulation and beach user perceptions on pocket beaches of Northern Sardinia

609 (Italy). *Ocean Coast Manag* 232, 106442.

610 Corrêa, M.R., Xavier, L.Y., Gonçalves, L.R., Andrade, M.M. de, Oliveira, M. de, Malinconico, N., Botero,

611 C.M., Milanés, C., Montero, O.P., Defeo, O., 2021. Desafios para promoção da abordagem

612 ecossistêmica à gestão de praias na América Latina e Caribe. *Estudos Avançados* 35, 219–236.

613 Costa, L.L., Fanini, L., Ben-Haddad, M., Pinna, M., Zalmon, I.R., 2022. Marine litter impact on sandy

614 beach fauna: A review to obtain an indication of where research should contribute more. *Microplastics*

615 1, 554–571.

616 da Silva, E.F., do Carmo, D. de F., Muniz, M.C., Dos Santos, C.A., Cardozo, B.B.I., de Oliveira Costa,

617 D.M., Dos Anjos, R.M., Vezzoni, M., 2022. Evaluation of microplastic and marine debris on the

618 beaches of Niterói Oceanic Region, Rio De Janeiro, Brazil. *Mar Pollut Bull* 175, 113161.

619 de Oliveira, C.R.S., da Silva Júnior, A.H., Mulinari, J., Ferreira, A.J.S., da Silva, A., 2023. Fibrous

620 microplastics released from textiles: Occurrence, fate, and remediation strategies. *J Contam Hydrol*

621 104169.

622 De Souza, R.B., Robinson, I.S., 2004. Lagrangian and satellite observations of the Brazilian Coastal

623 Current. *Cont Shelf Res* 24, 241–262.

624 Dos Santos, M., de Araújo Costa, I.P., Gomes, C.F.S., 2021. Multicriteria decision-making in the selection

625 of warships: a new approach to the AHP method. *International Journal of the Analytic Hierarchy*

626 *Process* 13.

- 627 dos Santos, V.R., Fávero, L.P.L., Moreira, M.Â.L., dos Santos, M., de Oliveira, L. de A., de Araújo Costa,
628 I.P., de Oliveira Capela, G.P., Kojima, E.H., 2023. Development of a computational tool in the Python
629 language for the application of the AHP-Gaussian method. *Procedia Comput Sci* 221, 354–361.
- 630 Fávero, L.P., Belfiore, P., 2017. *Manual de Análise de Dados: Estatística e Modelagem Multivariada com*
631 *Excel®, SPSS® e Stata®*. Elsevier, Rio de Janeiro, RJ, Brasil.
- 632 Ferraro, J.R., 2003. *Introductory raman spectroscopy*. Elsevier.
- 633 Ferreira, A.T. da S., Oliveira, R.C. de, Ribeiro, M.C.H., Grohmann, C.H., Siegle, E., 2023. Coastal
634 Dynamics Analysis Based on Orbital Remote Sensing Big Data and Multivariate Statistical Models.
635 *Coasts* 3, 160–174.
- 636 Ferreira, A.T. da S., Siegle, E., Ribeiro, M.C.H., Santos, M.S.T., Grohmann, C.H., 2021. The dynamics of
637 plastic pellets on sandy beaches: a new methodological approach. *Mar Environ Res* 163, 105219.
- 638 Franzen, M.O., Fernandes, E.H.L., Siegle, E., 2021. Impacts of coastal structures on hydro-morphodynamic
639 patterns and guidelines towards sustainable coastal development: A case studies review. *Reg Stud*
640 *Mar Sci* 44, 101800.
- 641 Fries, E., Dekiff, J.H., Willmeyer, J., Nuelle, M.-T., Ebert, M., Remy, D., 2013. Identification of polymer
642 types and additives in marine microplastic particles using pyrolysis-GC/MS and scanning electron
643 microscopy. *Environ Sci Process Impacts* 15, 1949–1956.
- 644 Gao, G.H.Y., Helm, P., Baker, S., Rochman, C.M., 2023. Bromine Content Differentiates between
645 Construction and Packaging Foams as Sources of Plastic and Microplastic Pollution. *ACS ES&T*
646 *Water* 3, 876–884.
- 647 Gao, Z., Wontor, K., Cizdziel, J. V, Lu, H., 2022. Distribution and characteristics of microplastics in beach
648 sand near the outlet of a major reservoir in north Mississippi, USA. *Microplastics and Nanoplastics* 2,
649 10.
- 650 GESAMP, 2019. Guidelines for the monitoring and assessment of plastic litter in the ocean, GESAMP
651 Reports & Studies.
- 652 Geyer, R., Jambeck, J.R., Law, K.L., 2017. Production, use, and fate of all plastics ever made. *Sci Adv* 3,
653 e1700782.
- 654 Ghosh, Shampa, Sinha, J.K., Ghosh, Soumya, Vashisth, K., Han, S., Bhaskar, R., 2023. Microplastics as an
655 emerging threat to the global environment and human health. *Sustainability* 15, 10821.
- 656 Göktuğ, T.H., 2021. Visitor-Sourced Pollution and Esthetic Quality in the Coastal National Parks: Sample
657 of Dilek Peninsula Büyük Menderes Delta National Park/Turkey. *Coastal Management* 49, 183–200.
- 658 Gramcianinov, C., Staneva, J., De Camargo, R., Silva Dias, P., 2023. Changes in extreme wave events in
659 the southwestern South Atlantic Ocean. *Ocean Dyn*.
- 660 Gunawan, N.R., Tessman, M., Zhen, D., Johnson, L., Evans, P., Clements, S.M., Pomeroy, R.S., Burkart,
661 M.D., Simkovsky, R., Mayfield, S.P., 2022. Biodegradation of renewable polyurethane foams in
662 marine environments occurs through depolymerization by marine microorganisms. *Science of The*
663 *Total Environment* 850, 158761.
- 664 Haberman, S.J., 1978. *Analysis of qualitative data: Introductory topics*. Academic Press, Incorporated, New
665 York, NY, New York.
- 666 Harari, J., De Camargo, R., França, C.A.S., Mesquita, A., Picarelli, S., 2006. Numerical Modeling of the
667 Hydrodynamics in the Coastal Area of Sao Paulo State Brazil. *J Coast Res* 39, 1560–1563.
- 668 Harris, P.T., 2020. The fate of microplastic in marine sedimentary environments: A review and synthesis.
669 *Mar Pollut Bull* 158, 111398.
- 670 Harris, P.T., Westerveld, L., Nyberg, B., Maes, T., Macmillan-Lawler, M., Appelquist, L.R., 2021.
671 Exposure of coastal environments to river-sourced plastic pollution. *Science of the Total Environment*
672 769, 145222.
- 673 Hartley, B.L., Thompson, R.C., Pahl, S., 2015. Marine litter education boosts children’s understanding and
674 self-reported actions. *Mar Pollut Bull* 90, 209–217.
- 675 Hidalgo-Ruz, V., Gutow, L., Thompson, R.C., Thiel, M., 2012a. Microplastics in the marine environment:
676 A review of the methods used for identification and quantification. *Environ Sci Technol* 46, 3060–
677 3075.
- 678 Hidalgo-Ruz, V., Gutow, L., Thompson, R.C., Thiel, M., 2012b. Microplastics in the Marine Environment:
679 A Review of the Methods Used for Identification and Quantification. *Environ Sci Technol* 46, 3060–
680 3075.

- 681 Hidalgo-Ruz, V., Thiel, M., 2013. Distribution and abundance of small plastic debris on beaches in the SE
682 Pacific (Chile): a study supported by a citizen science project. *Mar Environ Res* 87, 12–18.
- 683 Ivar do Sul, J.A., Costa, M.F., 2014. The present and future of microplastic pollution in the marine
684 environment. *Environmental Pollution* 185, 352–364.
- 685 Jambeck, J.R., Geyer, R., Wilcox, C., Siegler, T.R., Perryman, M., Andrady, A., Narayan, R., Law, K.L.,
686 2015. Plastic waste inputs from land into the ocean. *Science* (1979) 347, 768–771.
- 687 Johnson, R.A., Wichern, D.W., 1992. *Applied multivariate statistical analysis*, New Jersey.
- 688 Jong, M.-C., Tong, X., Li, J., Xu, Z., Chng, S.H.Q., He, Y., Gin, K.Y.-H., 2022. Microplastics in equatorial
689 coasts: Pollution hotspots and spatiotemporal variations associated with tropical monsoons. *J Hazard*
690 *Mater* 424, 127626.
- 691 Katsara, K., Kenanakis, G., Alissandrakis, E., Papadakis, V.M., 2022. Low-Density Polyethylene Migration
692 from Food Packaging on Cured Meat Products Detected by Micro-Raman Spectroscopy.
693 *Microplastics* 1, 428–439.
- 694 Kim, I.S., Chae, D.H., Kim, S.K., Choi, S.B., Woo, S.B., 2015. Factors Influencing the Spatial Variation
695 of Microplastics on High-Tidal Coastal Beaches in Korea. *Arch Environ Contam Toxicol* 69, 299–
696 309.
- 697 Laurino, I.R.A., Lima, T.P., Turra, A., 2023. Effects of natural and anthropogenic storm-stranded debris in
698 upper-beach arthropods: Is wrack a prey hotspot for birds? *Science of The Total Environment* 857,
699 159468.
- 700 Lavenère-Wanderley, A.A., Siegle, E., 2019. Wave-induced sediment mobility on a morphologically
701 complex continental shelf: eastern Brazilian shelf. *Geo-Marine Letters* 39, 349–361.
- 702 Lavers, J.L., Bond, A.L., 2017. Exceptional and rapid accumulation of anthropogenic debris on one of the
703 world’s most remote and pristine islands. *Proc Natl Acad Sci U S A* 114, 6052–6055.
- 704 Lebreton, L.C.M., Van Der Zwet, J., Damsteeg, J.-W., Slat, B., Andrady, A., Reisser, J., 2017. River plastic
705 emissions to the world’s oceans. *Nat Commun* 8, 15611.
- 706 Lefebvre, C., Le Bihanic, F., Jalón-Rojas, I., Dusacre, E., Chassaing, L., Bichon, J., Clérandeau, C., Morin,
707 B., Lecomte, S., Cachot, J., 2023. Spatial distribution of anthropogenic particles and microplastics in
708 a meso-tidal lagoon (Arcachon Bay, France): A multi-compartment approach. *Science of The Total*
709 *Environment* 898, 165460.
- 710 Löder, M.G.J., Gerdt, G., 2015. Methodology Used for the Detection and Identification of Microplastics—
711 A Critical Appraisal BT - Marine Anthropogenic Litter. In: Bergmann, M., Gutow, L., Klages, M.
712 (Eds.), . Springer International Publishing, Cham, pp. 201–227.
- 713 Mahiques, M.M. de, Siegle, E., Alcántara-Carrió, J., Silva, F.G., de Oliveira Sousa, P.H.G., Martins, C.C.,
714 2016. The Beaches of the State of São Paulo. In: Short, A.D., Klein, A.H.F. (Eds.), *Brazilian Beach*
715 *Systems*. Springer, Berlin, Germany, pp. 397–418.
- 716 Martin, J., Lusher, A., Thompson, R.C., Morley, A., 2017. The Deposition and Accumulation of
717 Microplastics in Marine Sediments and Bottom Water from the Irish Continental Shelf. *Sci Rep* 7,
718 1–9.
- 719 Mascagni, M.L., Siegle, E., Tessler, M.G., Y Goya, S.C., 2018. Morphodynamics of a wave dominated
720 embayed beach on an irregular rocky coastline. *Braz J Oceanogr* 66, 172–188.
- 721 McCreery, R.L., 2005. *Raman spectroscopy for chemical analysis*. John Wiley & Sons.
- 722 Möller Jr, O.O., Piola, A.R., Freitas, A.C., Campos, E.J.D., 2008. The effects of river discharge and seasonal
723 winds on the shelf off southeastern South America. *Cont Shelf Res* 28, 1607–1624.
- 724 Monico, J.F.G., 2008. *Posicionamento pelo GNSS: descrição, fundamentos e aplicações*, São Paulo. Editora
725 UNESP, São Paulo.
- 726 Monico, J.F.G., Dal Poz, A.P., Galo, M., Dos Santos, M.C., De Oliveira, L.C., 2009. Acurácia e precisão:
727 revendo os conceitos de forma acurada. *Boletim de Ciências Geodésicas* 15, 469–483.
- 728 Nelms, S.E., Duncan, E.M., Broderick, A.C., Galloway, T.S., Godfrey, M.H., Hamann, M., Lindeque, P.K.,
729 Godley, B.J., 2016. Plastic and marine turtles: A review and call for research. *ICES Journal of Marine*
730 *Science* 73, 165–181.
- 731 Nunes, L.H., Greco, R., Marengo, J.A., 2018. Climate change in Santos Brazil: Projections, impacts and
732 adaptation options, *Climate Change in Santos Brazil: Projections, Impacts and Adaptation Options*.
- 733 Ogata, Y., Takada, H., Mizukawa, K., Hirai, H., Iwasa, S., Endo, S., Mato, Y., Saha, M., Okuda, K.,
734 Nakashima, A., Murakami, M., Zurcher, N., Booyatumanondo, R., Zakaria, M.P., Dung, L.Q.,
735 Gordon, M., Miguez, C., Suzuki, S., Moore, C., Karapanagioti, H.K., Weerts, S., McClurg, T., Burres,

736 E., Smith, W., Velkenburg, M. Van, Lang, J.S., Lang, R.C., Laursen, D., Danner, B., Stewardson, N.,
737 Thompson, R.C., 2009. International Pellet Watch: Global monitoring of persistent organic pollutants
738 (POPs) in coastal waters. 1. Initial phase data on PCBs, DDTs, and HCHs. *Mar Pollut Bull* 58, 1437–
739 1446.

740 Oliveira, J., Belchior, A., da Silva, V.D., Rotter, A., Petrovski, Ž., Almeida, P.L., Lourenço, N.D.,
741 Gaudêncio, S.P., 2020. Marine environmental plastic pollution: mitigation by microorganism
742 degradation and recycling valorization. *Front Mar Sci* 7, 567126.

743 Peter A. Burrough, McDonnell, R.A., Lloyd, C.D., 1998. Principles of Geographical Information Systems.
744 Oxford University Press, New York, NY, USA.

745 Pianca, C., Mazzini, P.L.F., Siegle, E., 2010. Brazilian offshore wave climate based on NWW3 reanalysis.
746 *Braz J Oceanogr* 58, 53–70.

747 Ranjani, M., Veerasingam, S., Venkatachalapathy, R., Jinoj, T.P.S., Guganathan, L., Mugilarasan, M.,
748 Vethamony, P., 2022. Seasonal variation, polymer hazard risk and controlling factors of microplastics
749 in beach sediments along the southeast coast of India. *Environmental Pollution* 305, 119315.

750 Reid, J., Seiler, L., Siegle, E., 2022. The influence of dredging on estuarine hydrodynamics: Historical
751 evolution of the Santos estuarine system, Brazil. *Estuar Coast Shelf Sci* 279, 108131.

752 Rochman, Chelsea M., Browne, M.A., Halpern, B.S., Hentschel, B.T., Hoh, E., Karapanagioti, H.K., Rios-
753 Mendoza, L.M., Takada, H., Teh, S., Thompson, R.C., 2013. Policy: Classify plastic waste as
754 hazardous. *Nature* 494, 169–170.

755 Rochman, Chelsea M., Hoh, E., Kurobe, T., Teh, S.J., 2013. Ingested plastic transfers hazardous chemicals
756 to fish and induces hepatic stress. *Sci Rep* 3, 1–7.

757 Rochman, C.M., Kurobe, T., Flores, I., Teh, S.J., 2014. Early warning signs of endocrine disruption in adult
758 fish from the ingestion of polyethylene with and without sorbed chemical pollutants from the marine
759 environment. *Science of the Total Environment* 493, 656–661.

760 Royer, S.-J., Ferrón, S., Wilson, S.T., Karl, D.M., 2018. Production of methane and ethylene from plastic
761 in the environment. *PLoS One* 13, e0200574.

762 Ryan, P.G., Moore, C.J., Van Franeker, J.A., Moloney, C.L., 2009. Monitoring the abundance of plastic
763 debris in the marine environment. *Philosophical Transactions of the Royal Society B: Biological
764 Sciences* 364, 1999–2012.

765 Saaty, T.L., 2008. Decision making with the analytic hierarchy process. *International journal of services
766 sciences* 1, 83–98.

767 Schmuck, A.M., Lavers, J.L., Stuckenbrock, S., Sharp, P.B., Bond, A.L., 2017. Geophysical features
768 influence the accumulation of beach debris on Caribbean islands. *Mar Pollut Bull* 121, 45–51.

769 Silva, M.S., Guedes, C.C.F., da Silva, G.A.M., Ribeiro, G.P., 2021. Active mechanisms controlling
770 morphodynamics of a coastal barrier: Ilha Comprida, Brazil. *Ocean and Coastal Research* 69, e21004.

771 Smith, E., Dent, G., 2019. Modern Raman spectroscopy: a practical approach. John Wiley & Sons.

772 Smith, M., Love, D.C., Rochman, C.M., Neff, R.A., 2018. Microplastics in Seafood and the Implications
773 for Human Health. *Curr Environ Health Rep* 5, 375–386.

774 Sousa, P.H.G.O., Siegle, E., Tessler, M.G., 2013. Vulnerability assessment of Massaguáçu beach (SE
775 Brazil). *Ocean Coast Manag* 77, 24–30.

776 Souza, C.R. de G., 2012. Praias Arenosas Oceânicas Do Estado De São Paulo (Brasil): Síntese Dos
777 Conhecimentos Sobre Morfodinâmica, Sedimentologia, Transporte Costeiro E Erosão Costeira.
778 *Revista do Departamento de Geografia* 308–371.

779 Stein, L.P., Siegle, E., 2019. Santos beach morphodynamics under high-energy conditions. *Revista
780 Brasileira de Geomorfologia* 20, 445–456.

781 Stein, L.P., Siegle, E., 2020. Overtopping events on seawall-backed beaches: Santos Bay, SP, Brazil. *Reg
782 Stud Mar Sci* 40.

783 Suguio, K., Martin, L., Bittencourt, ACSP, Bittencourt, A, Dominguez, J., Flexor, A., 1985. Flutuações do
784 nível do mar durante o Quaternário superior ao longo do litoral brasileiro e suas implicâncias na
785 sedimentação costeira. *Revista Brasileira de Geociências* 15.

786 Suguio, K., Tessler, M.G., 1984. Planícies de cordões litorâneos do estado de São Paulo. *Boletim IG-USP
787 10*, 1–34.

788 Sun, X., Wang, T., Chen, B., Booth, A.M., Liu, S., Wang, R., Zhu, L., Zhao, X., Qu, K., Xia, B., 2021.
789 Factors influencing the occurrence and distribution of microplastics in coastal sediments: from source
790 to sink. *J Hazard Mater* 410, 124982.

791 Tessler, M., Goya, S., Yoshikawa, P.H., 2018. S. Erosão e Progradação do Litoral Brasileiro–São Paulo.
792 In: Muehe, D. (Ed.), Erosão e Progradação No Litoral Brasileiro. Dieter Muehe (Org.), Brasília,
793 MMA. MMA, Brasília, Brasil, pp. 297–346.

794 Teuten, E.L., Saquing, J.M., Knappe, D.R.U., Barlaz, M.A., Jonsson, S., Björn, A., Rowland, S.J.,
795 Thompson, R.C., Galloway, T.S., Yamashita, R., Ochi, D., Watanuki, Y., Moore, C., Viet, P.H., Tana,
796 T.S., Prudente, M., Boonyatumanond, R., Zakaria, M.P., Akkhavong, K., Ogata, Y., Hirai, H., Iwasa,
797 S., Mizukawa, K., Hagino, Y., Imamura, A., Saha, M., Takada, H., 2009. Transport and release of
798 chemicals from plastics to the environment and to wildlife. *Philosophical Transactions of the Royal*
799 *Society B: Biological Sciences* 364, 2027–2045.

800 Thompson, R.C., Olsen, Y., Mitchell, R.P., Davis, A., Rowland, S.J., John, A.W.G., McGonigle, D.,
801 Russell, A.E., 2004. Lost at sea: where is all the plastic? *Science* (1979) 304, 838.

802 Tian, W., Song, P., Zhang, H., Duan, X., Wei, Y., Wang, H., Wang, S., 2023. Microplastic materials in the
803 environment: Problem and strategical solutions. *Prog Mater Sci* 132, 101035.

804 Tiwari, M., Sahu, S.K., Rathod, T., Bhangare, R.C., Ajmal, P.Y., Pulhani, V., Kumar, A.V., 2023.
805 Comprehensive Review on Sampling, Characterization and Distribution of Microplastics in Beach
806 Sand and Sediments. *Trends in Environmental Analytical Chemistry* e00221.

807 Turra, A., Manzano, A.B., Dias, R.J.S., Mahiques, M.M., Barbosa, L., Balthazar-Silva, D., Moreira, F.T.,
808 2014. Three-dimensional distribution of plastic pellets in sandy beaches: shifting paradigms. *Sci Rep*
809 4.

810 Van Cauwenberghe, L., Devriese, L., Galgani, F., Robbins, J., Janssen, C.R., 2015. Microplastics in
811 sediments: A review of techniques, occurrence and effects. *Mar Environ Res* 111, 5–17.

812 Veerasingam, S., Ranjani, M., Venkatachalapathy, R., Bagaev, A., Mukhanov, V., Litvinyuk, D.,
813 Verzhavskaia, L., Guganathan, L., Vethamony, P., 2020. Microplastics in different environmental
814 compartments in India: Analytical methods, distribution, associated contaminants and research needs.
815 *TrAC Trends in Analytical Chemistry* 133, 116071.

816 Vito, D., Fernandez, G., Maione, C., 2022. A toolkit to monitor marine litter and plastic pollution on coastal
817 tourism sites. *Environ Eng Manag J* 21, 1721–1731.

818 Wang, C., Zhao, J., Xing, B., 2021. Environmental source, fate, and toxicity of microplastics. *J Hazard*
819 *Mater* 407, 124357.

820 Young, A., Elliott, J.A., 2018. Characterization of microplastic and mesoplastic debris in sediments from
821 Kamilo Beach and Kahuku Beach, Hawai'i Risk of Zoonotic Disease from a Wildlife Reservoir View
822 project.

823 Zeng, E.Y., 2023. Microplastic contamination in aquatic environments: an emerging matter of
824 environmental urgency. Elsevier.

825 Zhang, Y.-Q., Lykaki, M., Markiewicz, M., Alrajoula, M.T., Kraas, C., Stolte, S., 2022. Environmental
826 contamination by microplastics originating from textiles: Emission, transport, fate and toxicity. *J*
827 *Hazard Mater* 430, 128453.

828 Ziani, K., Ioniță-Mîndrican, C.-B., Mititelu, M., Neacșu, S.M., Negrei, C., Moroșan, E., Drăgănescu, D.,
829 Preda, O.-T., 2023. Microplastics: a real global threat for environment and food safety: a state of the
830 art review. *Nutrients* 15, 617.

831